



Full length article

Graphene oxide: A growth factor delivery carrier to enhance chondrogenic differentiation of human mesenchymal stem cells in 3D hydrogels



Mi Zhou^a, Neus Lozano^a, Jacek K. Wychowaniec^{b,c,1}, Tom Hodgkinson^a, Stephen M. Richardson^a, Kostas Kostarelos^d, Judith A. Hoyland^{a,e,*}

^a Division of Cell Matrix Biology and Regenerative Medicine, School of Biological Sciences, Faculty of Biology, Medicine and Health, University of Manchester, Manchester Academic Health Science Centre, Manchester, M13 9PT, UK

^b Manchester Institute of Biotechnology and School of Materials, The University of Manchester, Manchester, M1 7DN, UK

^c School of Materials, Faculty of Science and Engineering, The University of Manchester, Oxford Road, Manchester, M13 9PL, UK

^d Division of Pharmacy and Optometry, School of Health Sciences, Faculty of Biology, Medicine and Health, University of Manchester, Manchester Academic Health Science Centre, Manchester, M13 9PT, UK

^e NIHR Manchester Biomedical Research Centre, Manchester University NHS Foundation Trust, Manchester Academic Health Science Centre, Grafton St, M13 9WU Manchester, UK

ARTICLE INFO

Article history:

Received 25 January 2019

Received in revised form 21 June 2019

Accepted 15 July 2019

Available online 17 July 2019

Keywords:

Graphene Oxide
Growth factor delivery in 3D
3D cell containing scaffold
Mesenchymal stem cells
Chondrogenesis

ABSTRACT

Cartilage engineering with stem cells in 3D scaffolds is a promising future therapy to treat cartilage defects. One challenge in the field is to design carriers to efficaciously deliver biological factors in 3D scaffolds containing stem cells to appropriately guide differentiation of these cells in same scaffolds and promote specific tissue synthesis. Graphene-based 2D nanomaterials have recently attracted extensive interest for their biomedical applications as they can adsorb a plethora of biological molecules, thus offering high potential as delivery carriers. This study utilized graphene oxide (GO) flakes to adsorb transforming growth factor β 3 (TGF- β 3), which were then incorporated into a collagen hydrogel. Human mesenchymal stem cells (hMSCs) were encapsulated in the same gel and chondrogenic differentiation assessed. The study showed GO flakes adsorbed > 99% TGF- β 3 with < 1.7% release. Adsorbed TGF- β 3 retained a similar conformation to its dissolved counterpart (free protein) but importantly demonstrated greater conformational stability. Smad2 phosphorylation was promoted, and higher chondrogenic gene expression and cartilage-specific extracellular matrix deposition were achieved compared to exogenously delivering TGF- β 3 in culture media. Effects were sustained in long-term 28-day culture. The results demonstrate GO flakes as highly-efficient for delivering GFs in 3D to guide cells in the same scaffold and induce tissue formation. The ability of GO flakes to provide sustained local delivery makes this material attractive for tissue engineering strategies, in particular for regionally-specific MSC differentiation (e.g. osteochondral tissue engineering).

Statement of Significance

Cartilage engineering involving stem cells in 3D scaffolds is a promising future therapy to treat cartilage defects which can lead to debilitating conditions such as osteoarthritis. However, this field faces the challenge to design delivery carriers to efficaciously deliver biological factors inside these 3D cell-containing scaffolds for appropriately-guided cell differentiation. Graphene-based 2D nanomaterials offer high potential as delivery carriers, but to date studies using them to deliver biological factors have been restricted to 2D substrates, non-scaffold cell masses, or acellular 3D scaffolds. Our study for the first time demonstrated simultaneously incorporating both human mesenchymal stem cells (hMSCs) and GO (graphene oxide)-adsorbed growth factor TGF β 3 into a 3D scaffold, where GO-adsorbed TGF β 3 enhanced chondrogenic differentiation of hMSCs and cartilage-tissue synthesis throughout the scaffold without needing to repeatedly supply TGF β 3 exogenously.

© 2019 Acta Materialia Inc. Published by Elsevier Ltd. This is an open access article under the CC BY license (<http://creativecommons.org/licenses/by/4.0/>).

* Corresponding author.

E-mail address: judith.hoyland@manchester.ac.uk (J.A. Hoyland).

¹ Current address: School of Chemistry, University College Dublin, Belfield, Dublin 4, Ireland

1. Introduction

Cartilage defects, such as those caused by injury or as a consequence of diseases such as osteoarthritis, represent a substantial and growing socioeconomic burden [1,2]. Cartilage is known for its low self-repair capacity [3], but current therapies are aimed primarily at treating symptoms rather than being regenerative [4]. One promising future regenerative treatment strategy is tissue engineering with mesenchymal stem cells (MSCs) [5,6], which usually involves the essential tri-components [7] namely: 1) stem cells able to proliferate and differentiate into chondrocytes; 2) 3D scaffolds (such as hydrogels commonly used for engineering cartilage) to host and deliver cells [8]; and 3) the appropriate biological cues (e.g. growth factors (GFs)) that induce chondrogenesis [4,9]. The delivery of these biological cues in an effective manner is important to promote desirable tissue formation especially *in situ* [10]. Currently, many clinical trials administering GFs use concentrated doses and repeated GF injections [9]. The results have been generally disappointing since sustained presentation of active factors in target tissues are negatively affected by both denaturation of factors *in situ* and the inability to retain factors locally [9,11]. The only positive clinical outcomes originate from trials with a material carrier (e.g. a hydrogel) to deliver the factors [9], but this direct loading usually leads to a substantial initial burst release with little long-term delivery. Therefore, it becomes important to incorporate a second delivery carrier in a scaffold/hydrogel, which is specifically-designed to retain active factors longer term [12].

Common second delivery carriers involve secondary polymer matrices (e.g. PLGA micro or nano-particles) dispersed in a hydrogel; these polymeric particles physically encapsulate GFs and release them upon polymer degradation or external triggers such as pH [13,14]; or alternatively, carriers immobilize factors on their surfaces through electrostatic or hydrophobic interactions thus presenting factors for a sustained period in a 3D scaffold [9,12]. Some recent carrier studies include the use of Laponite nanoparticles to effectively adsorb and deliver GFs both *in vitro* and *in vivo* [15,16], and scaffolds modified to present affinity groups (e.g. sulphate) to adsorb and present GFs in 3D [17,18].

More recently, the newly-discovered 2D nanomaterial graphene (G) has attracted extensive interest for its applicability to tissue engineering in the biomedical field [19–21]. The studies unveiled interesting properties of G and its oxides (GO) in constructing cell substrates [22] and guiding specific cell functions including cellular differentiation. Several studies have reported enhanced or accelerated differentiation along a specific cell lineage [23–26], and one study has demonstrated that a GO-coated 2D substrate could enhance differentiation along multi-lineages including bone, adipose tissue and epithelium [27]. Although different aspects of G/GO properties are responsible for such effects, including its unique nano-topography, mechanical strength and electrical conductivity [25,26], the unique ability of G/GO to capture differentiation cues, e.g. GFs, from culture media and accumulate them onto their surface was one common reason for enhanced cell differentiation in several studies [23,27–30]. However, in such studies [23,27–30], differentiation cues were all supplied exogenously in culture media and unmonitored, thus the quantities of molecules adsorbed on G/GO and their distributions on or inside a substrate were largely uncontrolled. Nevertheless, such observations importantly indicate the potential for G/GO to act as a GF delivery carrier. In 2014, Wang and colleagues coated a titanium implant surface with GO to adsorb and deliver bone morphogenetic protein 2 (BMP2) into bone defects and promoted bone formation *in vivo* [24], and Yoon *et al.* used GO to deliver both transforming growth factor- β 3 (TGF- β 3) and fibronectin to adipose-derived MSC pellets, enhancing chondrogenesis [31].

To date, studies using (G/GO)-adsorbed growth factors to differentiate stem cells have been restricted to 2D or non-scaffold systems (e.g. pellet cultures), and studies using G/GO to deliver genes/drugs within a 3D system (e.g. a hydrogel) have been restricted to acellular systems [32,33]. Since sustainably delivering GFs to cells within 3D scaffolds is a crucial aspect for reconstructing tissue *in situ*, GO's potential as a GF delivery system in 3D to induce desirable cell function is an important aspect to be explored and may have huge potential in musculoskeletal tissue engineering/regenerative medicine.

In this study, utilising a collagen hydrogel as a model 3D scaffold, we demonstrate the ability of GO flakes to deliver the chondrogenic growth factor TGF- β 3 to promote chondrogenesis of human MSC (hMSC) with enhanced cartilage matrix formation. The method involved dispersion of GO-adsorbed TGF- β 3 into collagen gels together with encapsulated hMSCs. Chondrogenesis of hMSCs in the gel with GO-adsorbed TGF- β 3 was compared with the cell-encapsulated gel with TGF- β 3 routinely added in culture media ('exogenous supply').

2. Experimental

2.1. Fabrication of GO

GO was synthesised *via* a modified Hummers' method under endotoxin-free conditions as previously described [34,35]. Briefly, 0.8 g of graphite flakes were mixed with 0.4 g of sodium nitrate (Sigma-Aldrich, UK) in a round-bottom flask, followed by the slow addition of 18.4 mL of sulfuric acid 99.999% (Sigma-Aldrich, UK) under mild stirring. After a homogenized mixture was achieved, 2.4 g of potassium permanganate (Sigma-Aldrich, UK) were gradually added and the mixture maintained for 30 min. Thereafter, 37 mL of water for injection (Fresenius Kabi, UK) was progressively added in a dropwise manner. The temperature was monitored and kept at 98 °C for 30 min. The mixture was next diluted with 112 mL of water for injection (Fresenius Kabi, UK), and 12 mL of 30% hydrogen peroxide (Sigma-Aldrich, UK) added. The resulting mixture was purified by several centrifugation cycles at 7690g for 20 min until a viscous orange/brown gel-like layer of GO began to appear on at the pellet-supernatant interface at neutral pH. This layer was extracted carefully with warm water for injection (Fresenius Kabi, UK). Large GO flakes (l-GO) were thereby obtained as an aqueous suspension with a concentration of 2 mg/mL (pH 6–7).

Structural properties including lateral dimension and thickness of GO flakes were studied by optical microscopy, transmission electron microscopy (TEM), and atomic force microscopy (AFM). UV – vis and fluorescence spectroscopy were used to characterise the material's optical properties including the absorbance and fluorescence, respectively. Raman spectroscopy and ζ -potential measurements were used to define the material's surface properties. Thermogravimetric analysis (TGA) was also performed to examine the functionalization degree of GO flakes. X-ray photoelectron spectroscopy (XPS) was used to quantify the chemical composition of the GO sheets, C/O ratio, and the contribution of each individual functional group such as carboxylic, carbonyl, and epoxy groups to the overall oxidation state of GO.

2.2. Assessment of TGF- β 3 adsorption and release

Adsorption of TGF- β 3 onto GO flakes and its subsequent release were assessed. To adsorb TGF- β 3 onto GO, a 20 μ L aqueous solution containing 0.6 μ g TGF- β 3 (PeproTech, UK) was mixed with 80 μ L GO dispersion containing 3.5–14 μ g GO (the weight range of GO used in the assay was based on unpublished fluorescence

spectroscopy data). The amount of TGF- β 3 added (0.6 μ g) was equivalent to total exogenous supply for 1 mL gel during chondrogenic culture period. The mixture was incubated at 4 °C for 1 h, and then diluted with 900 μ L water. The diluted mixture was centrifuged at 12000g for 30 min leaving GO pellet with adsorbed TGF- β 3 at the tube bottom and supernatants were tested for un-adsorbed TGF- β 3 using a sandwich ELISA assay (BioTechnique, UK). The pellets after centrifugation were re-suspended in 1 mL water and incubated for 1, 2, 24, 48 and 72 h. The amount of released TGF- β 3 into water was measured at each time point using the same method. TGF- β 3 release beyond 72 h was estimated using mathematical modelling, which fitted the 72-hour data into a two-phase release including an initial burst release and afterwards a release following Fickian diffusion. The diffusion coefficients (D) in Phase II were calculated using non-steady Fickian diffusion [36] derived from Higuchi model [37] using Eq. (1):

$$\frac{M_t}{M_\infty} = \frac{4}{l} \sqrt{\frac{Dt}{\pi}} \quad (1)$$

where M_t is the amount (mass) of TGF- β 3 released at time t , M_∞ is the total amount (mass) of TGF- β 3 at $t = 0$, and l is the depth of the TGF- β 3 and GO mixture.

2.3. Assessment of GO-adsorbed TGF- β 3 conformation

The conformation (secondary structure) of GO-adsorbed TGF- β 3 was assessed using circular dichroism and compared with the conformation of TGF- β 3 in aqueous solution (a bioactive form of TGF- β 3 as reported in [38]). Samples were prepared by incubating mixtures of TGF- β 3 and GO, or solely TGF- β 3 (both in aqueous solutions) at 4 °C for 1 h and 7 days. Circular dichroism spectra were then measured using a ChiraScan[®] circular dichroism spectrometer (Applied Photophysics, UK) and data between wavelengths 180–260 nm recorded with a 0.5 nm bandwidth and a 5 s/point response time.

2.4. hMSC cell culture

hMSCs were isolated from the bone marrow of patients with osteoarthritis (age range: 25–73 years, average age: 54.6 years). Ethical approval was given by the North-West Research Ethics Committee, and patients were fully informed with written consent documented. Briefly, bone marrow removed during hip replacement surgery or knee arthroplasty were used to isolate hMSC cells as previously described [39], and isolated cells cultured in Minimum Essential Medium (Eagle's)-alpha modified (α MEM, Sigma, UK) with 20% (v/v) foetal bovine serum (FBS, Sigma, UK). Non-adherent cells were discarded after 5 days and adherent cells were cultured to confluence. The cluster of differentiation (CD) profile of MSCs (positive markers: CD73, CD90, and CD105; negative markers: CD34, CD45, CD11b, CD19 and HLA-DR) was analyzed using flow cytometry, and the ability of cells to differentiate along the three mesenchymal lineages was confirmed using standard differentiation methods [39]. For experiments, cells were further expanded in monolayer using α MEM with 10% (v/v) FBS and 10 μ M ascorbic acid (hMSC growth media). Cells at passage 3–4 were used in experiments with each experiment repeated with 3 patients' samples ($n = 3$).

2.5. Cytotoxicity assessment

Cell-encapsulated collagen-GO hybrid gels were cultured in hMSC growth media for 14 days and cell viability assessed with a Live/Dead[®] Viability assay (Thermo-Scientific, UK). Stained cells were imaged using an Olympus B51 fluorescence microscope at

an excitation wavelength of 495 nm with two emission wavelengths at 515 and 635 nm, respectively. To further assess the effect of direct GO exposure, hMSCs cultured on glass cover slips (5×10^4 cells/cm² of glass) were exposed to 10 ng/mL GO in culture media for 72 h with cell viability measured using the same assay.

2.6. Preparation of cell-encapsulated Collagen-GO hybrid gels containing GO adsorbed TGF- β 3

To prepare the hybrid gels, TGF- β 3 in aqueous solution and aqueous dispersion of GO flakes were incubated together at 4 °C for 1 h. The mixture was then added into a pH 7 collagen solution (with 97% type I collagen from bovine skin, Collagen Solutions, UK) and vortexed to achieve homogeneity. hMSCs were encapsulated into the collagen-GO (with adsorbed TGF- β 3) mixture to a final cell density of 4×10^6 /mL and 100 μ L aliquots were dispensed into 24-well culture inserts and incubated at 37 °C for 30 min to form cell-encapsulated gels (Fig. 1). The cast gels were 3.3 mm-high cylinders with base diameter of 6.6 mm. In the study, final collagen concentration was fixed at 3.0 mg/mL (of gel), and GO and TGF- β 3 concentrations were 600 μ g/mL and 0.6 μ g/mL respectively, unless specifically stated. Aqueous dispersions of GO flakes (6–600 μ g/mL) were used for assessing: i) cytotoxicity of the hybrid gels and ii) influence of GO concentration on TGF- β 3 delivery efficacy with TGF- β 3 concentration fixed at 0.6 μ g/mL. Alternatively, TGF- β 3 concentrations of 0.1–0.4 μ g/mL (of gel) were used to assess the effect of lower doses of TGF- β 3 adsorbed to GO on chondrogenesis.

2.7. Assessment of GO uptake into cells

The cell-encapsulated gels were fixed at day 14 in 4% paraformaldehyde/2.5% glutaraldehyde (pH 7.2), and post-fixed in 1% osmium tetroxide/1.5% potassium ferrocyanide (pH 7.2). Gels were incubated with 1% uranyl acetate in water, dehydrated by ethanol and embedded into TAAB 812 resin. Thin sections were visualized using an FEI[®] Tecnai 12 Biotwin transmission electron microscope (TEM) at an accelerating voltage of 100 kV and imaged using an Orius SC1000 CCD camera (Gatan, US).

2.8. Chondrogenic differentiation of gel-encapsulated hMSC cells

To assess chondrogenic differentiation, the cell-encapsulated gels containing GO-adsorbed TGF- β 3 were cultured in chondrogenic media without TGF- β 3; media contained Dulbecco's modified Eagle's Medium (DMEM) supplemented with 100 μ M ascorbic acid, 1.25 mg/mL bovine serum albumin (BSA, AlbuMax[®], Thermo-Fisher Scientific, UK), 10^{-7} M dexamethasone, 1% (v/v) FBS, and a mixture of insulin-transferrin-selenium (insulin: 10 μ g/mL, transferrin: 5.5 μ g/mL, selenium: 6.7 ng/mL; Gibco[®], Thermo-Fisher Scientific, UK), 40 μ g/mL L-proline and 5.4 μ g/ml linoleic acid (ingredients were from Sigma, UK unless indicated). For gels without GO-adsorbed TGF- β 3, constructs were cultured in the above chondrogenic media with TGF- β 3 added exogenously at a concentration of 10 ng/mL every two days when the medium was replaced.

2.8.1. Assessment of Smad signaling

Cell-encapsulated gels were placed in RIPA buffer containing phosphatase and protease inhibitors, vortexed and centrifuged to extract protein according to manufacturer's instructions (Thermo-Fisher Scientific, UK). Protein was quantified using the BCA assay (Pierce ThermoFisher Scientific) and 30 μ g protein from each sample loaded into the wells of a Bolt 4–12% Bis-Tris Plus Gels (ThermoFisher Scientific) and gel electrophoresis performed.

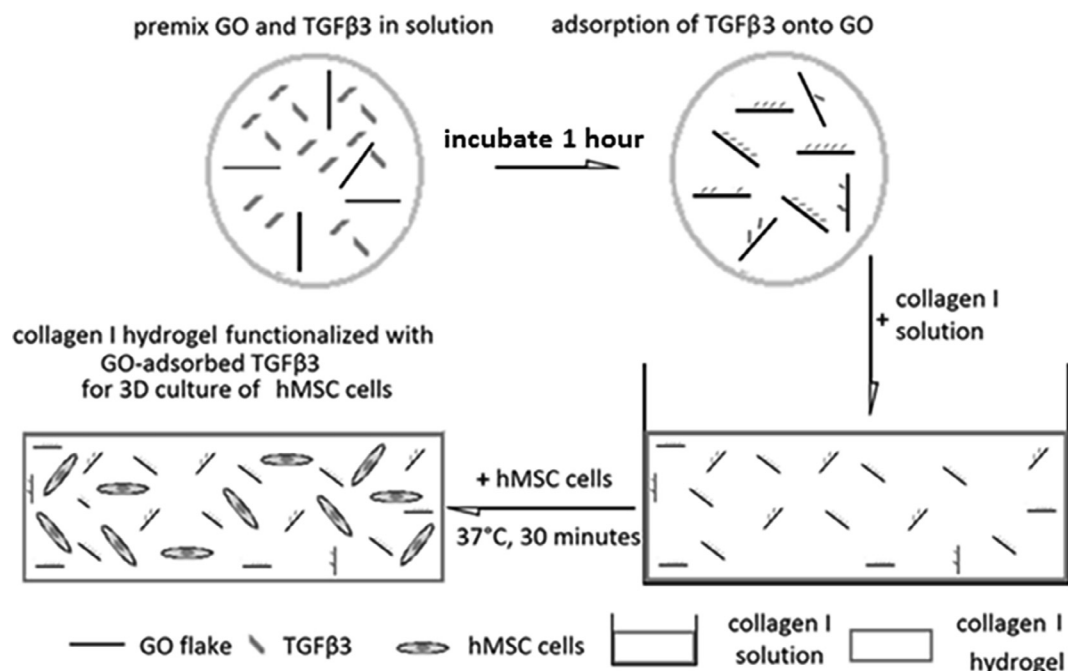


Fig. 1. The procedure for preparing cell-encapsulated Collagen-GO hybrid gels containing GO adsorbed TGF- β 3 (TGF β 3).

Separated proteins were then transferred to a polyvinylidene difluoride (PVDF) membrane and blocked for one hour at room temperature with blocking buffer (5% (w/v) bovine serum albumin (BSA) in TBS with 0.1% (v/v) Tween20 (TBST)). After blocking, membranes were incubated with primary antibodies against phospho-Smad2 (1:1000 dilution), Smad2 (1:1000 dilution) or GAPDH (1:10000 dilution) (Millipore, UK) diluted in blocking buffer overnight at 4 °C with gentle agitation. Membranes were washed 5 times with TBST and further probed with relevant HRP-conjugated secondary antibodies (1:10000 dilution in blocking buffer) (antibodies from Cell Signalling Technology, US unless indicated) for 1 h at room temperature. After incubation membranes were washed again 5 times with TBST. Protein bands were visualised by incubation with ECL Plus reagent (Pierce, US) and exposure to photographic film.

2.8.2. Analysis of chondrogenic gene expression

To analyse the expression of chondrogenic genes, cell-encapsulated gels at day 14 and 28 were disrupted in TRIzol[®] and RNA was extracted according to the manufacturer's instructions (Geno Technology, US). Extracted RNA was reverse transcribed with a high-capacity reverse transcription kit (Thermo-Fisher Scientific, UK). Chondrogenic gene expression was measured by quantitative real-time PCR (qPCR) using an Applied Biosystems[®] StepOnePlus[™] Real-Time PCR system. Reactions were prepared in triplicate by using LuminoCt qPCR ReadyMix reagents (Sigma-Aldrich, UK) to a total volume of 10 μ L, containing 10 ng cDNA, 900 nM each primer, and 250 nM probe. Data were analyzed according to the $2^{-\Delta\Delta Ct}$ method [40] and normalized to pre-validated reference gene EIF2B1. The primers and probes used for qPCR analysis are detailed in Suppl. Table 1.

2.9. Histological analysis of cartilage-specific ECM

Gels at day 28 were fixed in 4% paraformaldehyde/PBS, dehydrated and then embedded in paraffin wax. Sections were cut at 5 μ m, mounted and stained with 1% alcian blue solution in 3% acetic acid (pH 2.5) (Alcian Blue-8GX, Sigma-Aldrich, UK). The stained sections were imaged using an EVOS XL Core microscope and intensity of the blue staining was measured using ImageJ

software (National Institutes of Health, USA). To assess type II collagen expression, sections were incubated with an anti-type II collagen primary antibody (rabbit polyclonal, Abcam, UK) and then a biotinylated goat anti-rabbit secondary antibody (Vector Labs, USA). Afterwards the sections were incubated with avidin-biotin complex solution (Vector Labs, USA) and then treated with 3,3'-Diaminobenzidine (DAB) substrate (Vector Labs, USA). The stained sections were also imaged using the EVOS XL Core microscope.

2.10. Assessment of gel rheology

Gels on day 28 were measured using a Bohlin C-VOR rheometer in an oscillatory mode. Each gel was placed between a 20 mm/2° cone plate and a flat stationary plate, and the gap between the two plates set as 100 μ m. A combined measurement including an 'amplitude sweep' and a 'frequency sweep' was performed. The 'amplitude sweep' was performed by applying controlled stresses that were linearly increased from 1.0 to 50 Pa and strains corresponding to the stresses were recorded; the oscillatory frequency was maintained at 1 Hz. The maximum strain within the linear visco-elastic region was chosen from the 'amplitude sweep' for the 'frequency sweep', in which the stress is altered to obtain the chosen strain. The elastic (G') and viscous moduli (G'') were measured as a function of frequency between 0.1 and 10 Hz, and G' at 1 Hz was used to represent gel stiffness.

2.11. Statistical analysis

For statistical analysis, two-tailed Student's t-tests assuming unequal variance were used to compare between samples, and P values of < 0.05 was considered as significantly different.

3. Results

3.1. Characteristics of fabricated GO

The produced aqueous dispersion of GO flakes was visually homogenous and of a yellow/brownish colouration. A summary of the GO flake characterisation is presented in Fig. 2. The

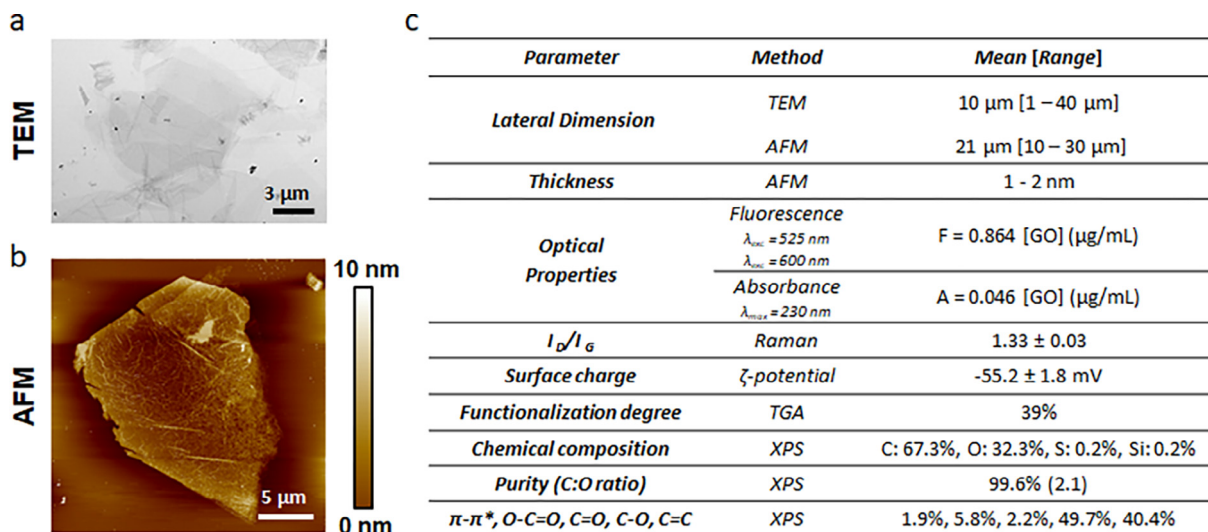


Fig. 2. Physicochemical characterisation of graphene oxide flakes. a-b) Representative TEM (a) and AFM (b) micrographs of GO sheets. c) Summary table illustrating the full physicochemical characterisation of GO flakes.

morphological features of GO flakes were examined using TEM and AFM. Both techniques demonstrated that the lateral dimensions of GO flakes ranged between 10 and 40 µm, and AFM demonstrated that these flakes were single to few layers thick (Fig. 2a-b). The surface properties were studied by Raman spectroscopy and ζ-potential measurement (Fig. 2c). Raman spectroscopy showed that GO displayed the characteristic G and D scatter bands present at 1595 cm^{-1} and 1320 cm^{-1} respectively, with an I_D/I_G ratio of approximately 1.3. ζ-potential measurement evidenced that the surface charge of GO was approximately -55 mV. Both TGA and XPS were performed to decipher the material's C/O ratio and chemical purity, and the nature and extent of functionalisation. The results indicate that the GO produced here had a high chemical purity (>99.5%), and a high degree of oxidation (C/O = 2.1) (Fig. 2c). The XPS high-resolution C1s spectrum further supports the extensive oxidation of graphite to yield GO flakes, with various oxygen-containing functionalities including carboxylic acid, carbonyl and hydroxyls/epoxide functional groups.

3.2. TGF-β3 adsorption onto and release from GO

Adsorption of TGF-β3 onto GO occurred when mixing the two in water. For 0.6 µg TGF-β3, which is the total amount used to exogenously supply 1 mL of cell-encapsulated gel for chondrogenesis, a few µg of GO flakes (3.5–14 µg) were able to adsorb >99% (Fig. 3a), leaving <1% as free TGF-β3 in aqueous phase as detected by ELISA. The GF was stably adsorbed and the release from GO flakes into water was <0.35% over 72 h (Fig. 3b).

The release of TGF-β3 from GO over longer term was further assessed using a mathematical model. Extrapolated from the 72-hour experimental data, the release of TGF-β3 was considered to occur in two successive phases: the initial burst release (Phase I, 0–2 h) and subsequently the diffusion phase (Phase II). The diffusion coefficients D in Phase II calculated using Eq. (1) (Section 2.2) were $<10^{-11}$ (Suppl. Table 2). Therefore, for a 28-day period, which is the time used in long term *in vitro* chondrogenesis, the estimation of release using above equation was <1.72%.

3.3. Conformation of GO-adsorbed TGF-β3

Circular dichroism measurements after 1-hour incubation revealed similar protein secondary structures for both TGF-β3

and GO-adsorbed TGF-β3 (Fig. 3c). Both secondary structures also resembled the previously-reported TGF-β3 structure when the molecule is active [38]. After 7 days, a change in spectra from day 0 was detected (Fig. 3c), specifically at the wavelength of 193 nm, which was the negative maximum assigned to protein random coil structure [41]. Noticeably at this negative maximum, this change (as θ in mdeg) from day 0 and 7 ($\Delta\theta = \theta_{\text{day7}} - \theta_{\text{day0}}$) was larger for TGF-β3 alone compared to its GO-adsorbed counterpart.

3.4. Cytotoxicity of collagen-GO hybrid gel

Cytotoxicity of collagen-GO hybrid gels were tested on hMSCs encapsulated in gels containing 6–600 µg/mL (of gel) GO. The hybrid gels appeared homogenous with uniform distribution of GO (Fig. 4a), and cells were evenly distributed after encapsulation into the gel (Fig. 4b, green: living cells; red: dead cells); cell viability was >99% during 14-day culture (Fig. 4b and c 1 day and 14 days post culture). In a separate study, 2D-cultured hMSCs (cells on glass) were directly exposed to GO flakes suspended in culture media, and cell viability also remained over 99% (Suppl. Fig. 1). TEM sections of the cell-containing gels revealed many cells in close proximity to GO flakes (Fig. 4d) but cell internalisation of GO was rare. No cells were found with apoptotic morphology, e.g. with chromatin condensation and plasma membrane blebbing.

3.5. Chondrogenic differentiation at 14 days

Western blotting was first used to assess Smad2 phosphorylation in response to TGF-β3 signalling. At 1-hour post cell encapsulation, phosphorylated-Smad2 was significantly higher in the gel containing GO-adsorbed TGF-β3 ('TGF-β3 + GO') than in the gel with exogenously-supplied TGF-β3 ('TGF-β3') (Fig. 4e & f, $p < 0.05$). After 14-day culture, chondrogenic gene expression (genes SOX9, COL2A1 and ACAN) assessed by qPCR was significantly higher in the former ('TGF-β3 + GO') compared to the latter ('TGF-β3'), but this only occurred when GO-concentration in the gel was more than 60 µg/mL. In fact, with different GO concentrations of 6–600 µg/mL for a same TGF-β3 concentration (0.6 µg/mL in the gel), increasing GO concentration resulted in proportionally-increased chondrogenic gene expression (Fig. 4g). When GO concentration reached 60 µg/mL, all 3 genes were expressed at

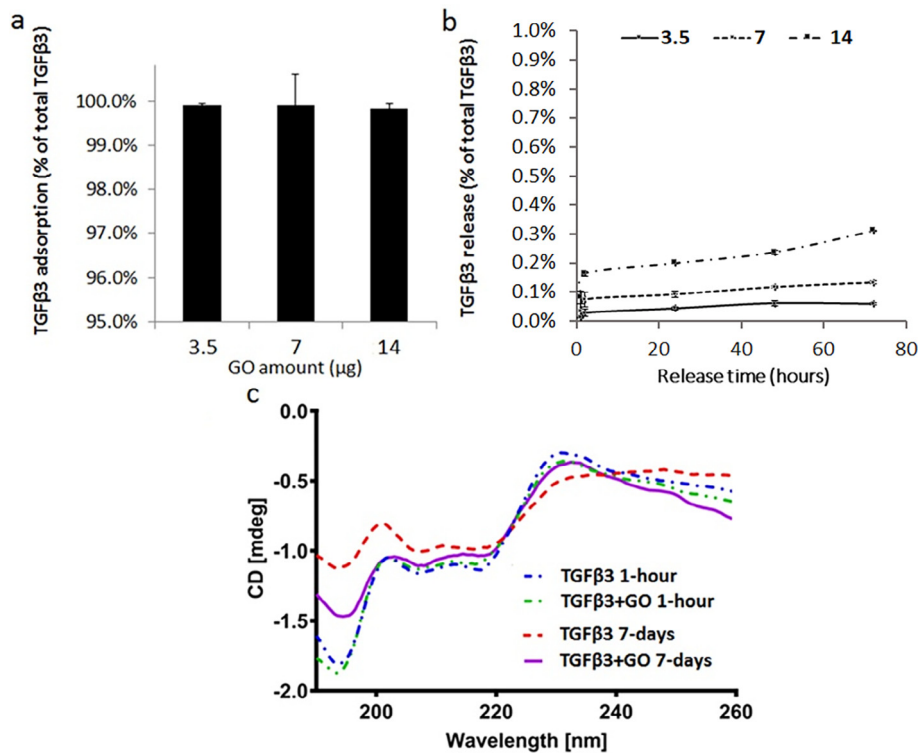


Fig. 3. TGF- β 3 adsorption onto GO, its subsequent release and the conformation (as secondary structure) of GO-adsorbed TGF- β 3 (TGF β 3). a) 99% of 0.6 μ g TGF- β 3 could be adsorbed onto 3.5–14 μ g GO. b) The release of TGF- β 3 from GO was <0.35% over 72 h. c) Secondary structures (shown by circular dichroism spectra) of TGF- β 3 and GO-adsorbed TGF- β 3 were similar at 1 h; at day 7 a spectra change was detected specifically at 193 nm wavelength (characteristic negative maximum for protein random coil), with the change more pronounced for TGF- β 3 alone.

comparable levels to exogenously supplying TGF- β 3 ($p > 0.05$); and at higher 300–600 μ g/mL GO, gene expression was significantly higher than exogenously supplying TGF- β 3 ($p < 0.01$). Without TGF- β 3, the collagen hydrogel either with or without GO, did not induce expression of SOX9 or ACAN at day 14, although COL2A1 was increased compared to day 0 but the increased level was statistically lower than having TGF- β 3 supplied (Suppl. Fig. 2).

3.6. Long-term (28-day) chondrogenic differentiation and ECM formation

The cultures were then extended to 28 days to understand longer term outcome of having TGF- β 3 pre-loaded in the gel via GO. GO concentration used in this assessment was 600 μ g/mL in the gel selected from the results of the 14-day culture. Similar to 14 days, 28-day chondrogenic gene expression remained significantly higher in the gel containing GO-adsorbed TGF- β 3 ('TGF β 3 + GO') compared to the gel with TGF- β 3 exogenously supplied ('TGF β 3') (Fig. 5a). Alcian blue, which stains glycosaminoglycans (GAG) to indicate formation of cartilage-specific ECM, also stained more intensely in the gel containing GO-adsorbed TGF- β 3 compared to the gel with TGF- β 3 exogenously supplied (Fig. 5b and c). The average stain intensity was calculated as 20% more intense in the former gel ($p < 0.05$). Immunohistochemical staining also showed expression of type II collagen in gels with GO-adsorbed TGF- β 3 (GO + TGF β 3) and staining intensity appeared more intense when compared to gels with TGF- β 3 supplied in media ('TGF β 3') (Fig. 5e and f). The gel containing GO but without any type of TGF- β 3 supply (Fig. 5a, 'GO') did not induce an increase in SOX9 expression when comparing day 28 data to day 0. Also, comparing it to the gel containing GO-adsorbed TGF- β 3, expression of chondrogenic genes were all significantly lower ($P < 0.01$). GAG or type II collagen staining in this gel was also not detectable in gels

containing only GO (Fig. 5d, g). At day 28, gel stiffness presented as elastic modulus G' were significantly higher for gels with GO-adsorbed TGF- β 3 (TGF β 3 + GO) compared to both gels with TGF- β 3 supplied in media (TGF β 3) and gels containing GO but without a TGF- β 3 supply (GO). (** $P < 0.01$).

Over the 28 days, ALPL (alkaline phosphatase) as an osteogenic gene marker did not increase in any gels (Suppl. Fig. 3a). Furthermore, addition of β -glycerophosphate for 21 days did not induce mineralization as no alizarin red staining was detectable. (Suppl. Fig. 3b).

3.7. Potential to lower TGF- β 3 dosage when delivered in gel using GO

All above experiments used a fixed TGF- β 3 concentration (0.6 μ g/mL) delivered by GO in the gel, which was equivalent to the amount exogenously delivered. GO-adsorbed TGF- β 3 was reduced to 0.4, 0.2 and 0.1 μ g/mL in the gel to assess if a lower concentration of GF could be used without compromising efficacy. It was found that 0.6 and 0.4 μ g/mL induced comparable levels of chondrogenesis (Fig. 6a) and GAG deposition (Fig. 6b and c). Reducing TGF- β 3 to 0.2 μ g/mL resulted in lower expression of SOX9 ($p < 0.01$), and 0.1 μ g/mL significantly decreased expression of all 3 genes and GAG deposition was significantly reduced ($p < 0.01$ compared to 0.6 μ g/mL, Fig. 6a, b, d).

4. Discussion

This study explored GO's capacity to retain and deliver biomolecules (in this case TGF- β 3) in a 3D cell-containing scaffold, which differs from previous work where acellular matrix [32,33], non-matrix (e.g. cell pellet culture [31]) or 2D systems [23–27] were utilised. Our study incorporated GO flakes with adsorbed TGF- β 3

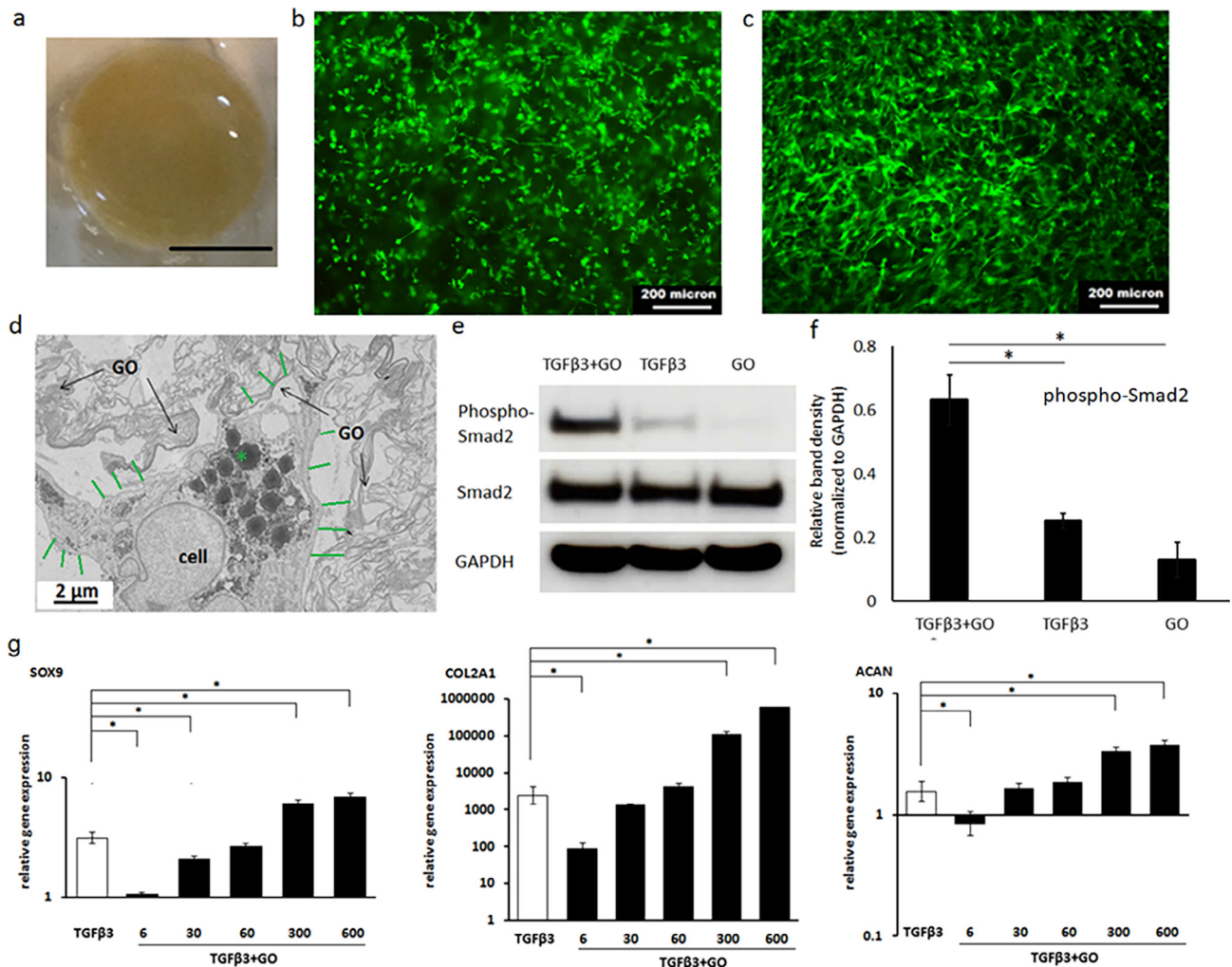


Fig. 4. Gel cytotoxicity, Smad2 phosphorylation and influence of GO concentrations on delivering TGF- β 3 in gel to direct chondrogenesis. a) Collagen-GO hybrid gel with 600 μ g/mL GO showed a uniform dispersion of GO (Scale: 500 μ m). b-c) hMSCs in collagen-GO hybrid gels maintained >99% viability after 1-day (b) and 14-day (c) culture (green: living cells, red: dead cells). d) Representative TEM image shows part of a cell (short green lines point to outline of the cell) in close proximity to GO flakes with no uptake of GO observed. (GO appeared as grey wavy structures) (* indicated oil bodies in the cell). e-f) Western blots showed higher expression of phosphorylated Smad2 with the gel containing GO-adsorbed TGF- β 3 (GO + TGF β 3) compared to TGF- β 3 exogenously supplied in media (TGF β 3). Without TGF- β 3 supply, Smad2 phosphorylation was not detected in GO-containing gel (GO). g) With increasing GO concentration in the gel, expression of chondrogenic genes (SOX9, COL2A1, and ACAN) increased proportionally (6–600 in the ‘TGF β 3 + GO’ group depict GO concentrations in μ g/mL (of gel) to adsorb and deliver 0.6 μ g/mL (of gel) TGF- β 3 in gel, and ‘TGF β 3’ depicts adding TGF- β 3 exogenously in media to supply a gel). Data is expressed as fold changes in gene expression relative to day 0 (‘D0’) (the time before cell encapsulation). N = 3. *P < 0.01 relative to ‘TGF β 3’ (depicting exogenous TGF- β 3 in media). (For interpretation of the references to colour in this figure legend, the reader is referred to the web version of this article.)

into a collagen hydrogel, and simultaneously encapsulated hMSC cells in the same gel, and assessed chondrogenesis.

Preparation of the hybrid gel containing GO-adsorbed TGF- β 3 and hMSC cells was simple. The initial mixing of TGF- β 3 with GO led to TGF- β 3 adsorption. GO has previously been shown to have strong affinity to proteins and peptides and therefore adsorbs a variety of these molecules. Adsorption occurs through long-range electrostatic attraction to positive charges on lysine and arginine in proteins, and also through short range hydrophobic and π - π stacking interactions (e.g. phenylalanine) as previously shown by ourselves [42] and others [31]. Also, due to their large surface area, GO flakes can adsorb large quantities of molecules to their surface [21,28], meaning only a few μ g of GO was needed in this study to adsorb a TGF- β 3 quantity equivalent to the total supplied exogenously. TGF- β 3 appeared to be stably adsorbed on GO as shown by the negligible release (<0.35%) over 72 h, similar to that previously reported [30]. Furthermore, mathematical modelling demonstrated that release would be < 1.72% in 28 days.

Conformation (secondary structure) of GO-adsorbed TGF- β 3 was examined and no secondary structure change was found after adsorption on GO compared to free TGF- β 3 in aqueous phase. Importantly, the conformation of GO-adsorbed TGF- β 3 resembled the active conformation previously reported using the same circular dichroism technique [38]. Within 7 days, there was a clear deterioration in secondary structure for free TGF- β 3 molecules in aqueous phase. This potentially indicates that the molecules gradually denatured losing their active form. Interestingly, GO-adsorbed TGF- β 3 had a slower deterioration in its secondary structure; and thus, GO potentially facilitated the retention of TGF- β 3 in active form as has been previously reported for GO-adsorbed insulin [30] or PEGylated GO-adsorbed BSA [43] which protected the growth factor from enzymatic degradation. The retained conformation after GO adsorption ensured that TGF- β 3 remained functional, which was evidenced by the fact that the adsorbed TGF- β 3 induced greater Smad2 phosphorylation in hMSCs than that seen with TGF- β 3 added exogenously to the cultures.

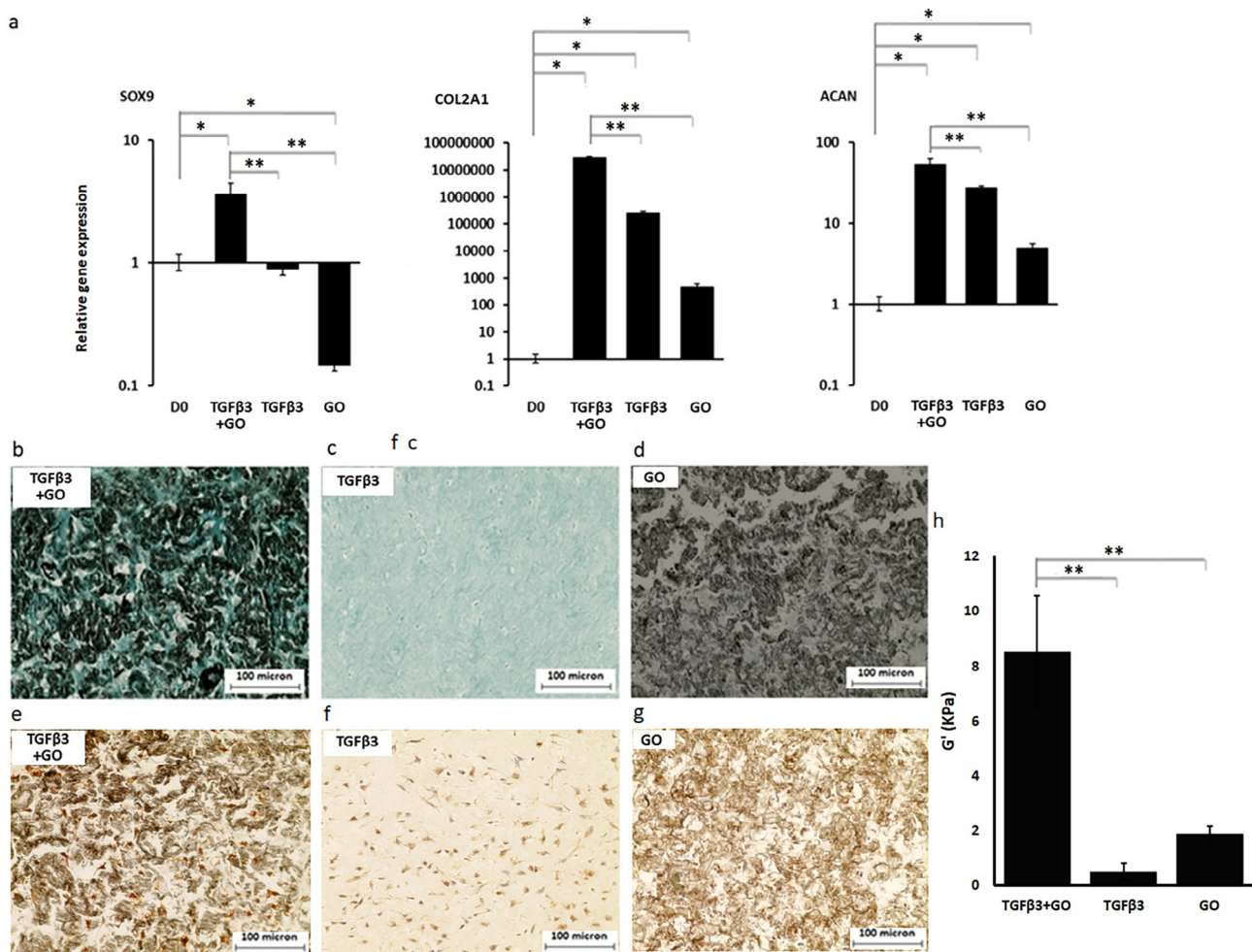


Fig. 5. Chondrogenic gene expression, GAG deposition, and gel stiffness after 28-day culture. a) At day 28, expression of chondrogenic genes (SOX9, COL2A1, and ACAN) were significantly higher in gels with GO-adsorbed TGF-β3 (TGFβ3 + GO) than in gels where TGF-β3 was supplied in media (TGFβ3). Data are expressed as fold changes in gene expression relative to day 0 ('D0'). N = 3. *P < 0.01 relative to 'D0' samples, **P < 0.01 relative to 'TGFβ3 + GO' samples. b-d) Alcian blue staining at day 28 for GAG deposition showed higher staining intensity in gels with GO-adsorbed TGF-β3 (TGFβ3 + GO, b) compared to gels with TGF-β3 supplied in media (TGFβ3, c), and staining was not detectable in gels containing GO only (GO, d). e-g) immunohistochemical staining at day 28 showed type II collagen deposition in gels with GO-adsorbed TGF-β3 (GO + TGFβ3, e) and the orange-brown staining (especially surrounding cells) was more prominent compared to gels with TGF-β3 supplied in media (TGFβ3, f); staining was not detected in gels containing GO only (GO, g). h) Gel stiffness (presented as elastic modulus G') were significantly higher at day 28 for gels with GO-adsorbed TGF-β3 (TGFβ3 + GO) compared to gels with TGF-β3 supplied in media (TGFβ3) and gels containing GO but without a TGF-β3 supply (GO). (**P < 0.01). (For interpretation of the references to colour in this figure legend, the reader is referred to the web version of this article.)

The study observed that gels containing 6–600 μg/mL GO were non-toxic to hMSCs. The lateral dimension of GO flakes was relatively large (10–40 μm), and this potentially prevented internalization of the flakes by cells. With the different GO concentrations used to deliver the same concentration of TGF-β3 in the gel (0.6 μg/mL of gel), different levels of chondrogenic gene expression was observed. High concentrations GO (300–600 μg/mL) were necessary to induce a significantly higher level of chondrogenesis compared to exogenously supplying the GF. Assuming a gel volume containing one cell as a unit volume, an increase in GO concentration would increase the probability of having GO flakes (with adsorbed TGF-β3) in that volume unit and hence in close proximity to the cell. The even distribution of GO flakes throughout the gel also avoids the issues associated with exogenous supply of GFs to gels, such as size or porosity of the gel, and molecular size and charge of the GF which can lead to compromised GF delivery in 3D scaffolds as reviewed by Lee and Ikada [9,10]. With 600 μg/mL GO to distribute 0.6 μg/mL TGF-β3 into gels at the beginning of the culture, the enhanced chondrogenesis was sustained over long-term 28 days, with increased cartilage matrix

formation evidenced by GAG staining (alcian blue), type II collagen staining and gel rheology.

Our data also illustrates that with our optimised system, in which 600 μg/mL GO was used to pre-adsorb and deliver TGF-β3 to the gel with 4×10^6 cells/mL hMSCs encapsulated, TGF-β3 concentration can be reduced without compromising overall chondrogenesis in the 3D construct. Similar results have been reported with laponite nanoparticles [15,16]. As such, these nanomaterials provide opportunities to use lower GF concentrations for clinical applications, thereby reducing costs and potentially side effects of excess GFs [9].

5. Conclusions

This study has shown that GO-adsorbed TGF-β3 can be dispersed into 3D gels together with hMSCs to effectively induce chondrogenesis. Gene expression and matrix analysis showed that levels of chondrogenesis with GO-adsorbed TGF-β3 in gels was higher than that seen when exogenously adding TGF-β3 to media.

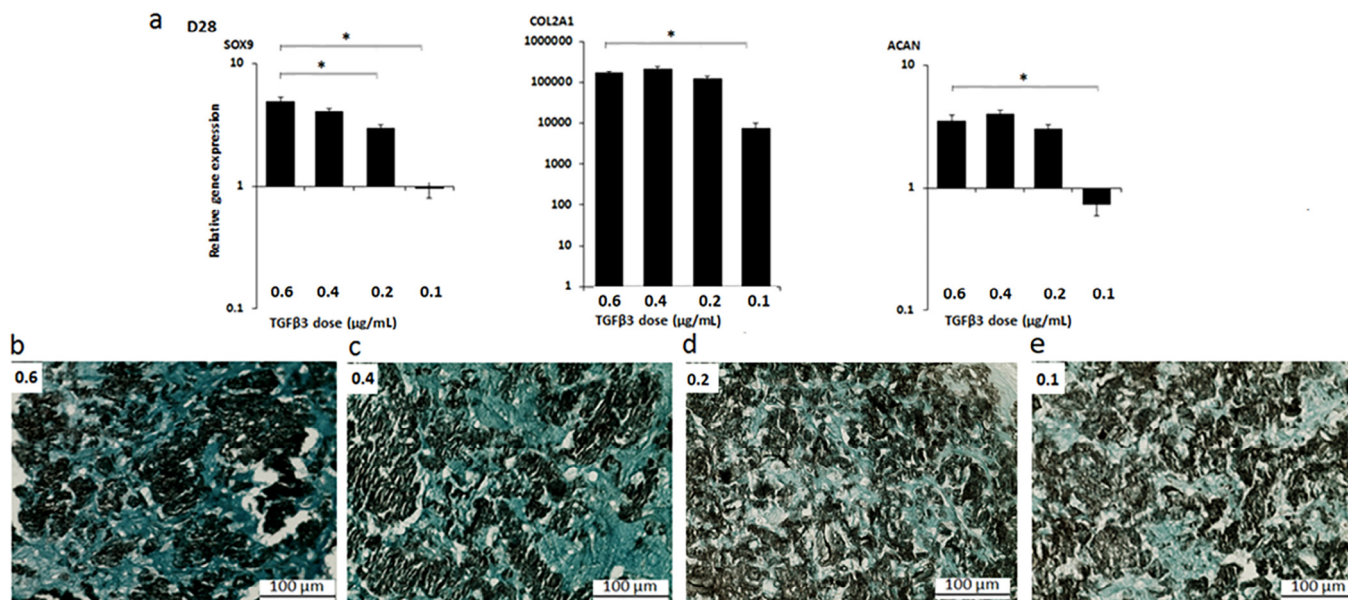


Fig. 6. Chondrogenesis with lower dose of TGF- β 3 adsorbed on GO. a) Chondrogenic gene expression was statistically similar in gels with 0.6 and 0.4 μ g/mL GO-adsorbed TGF- β 3 (TGF β 3) while 0.1 μ g/mL led to significantly lower gene expression. Data is expressed as fold changes in gene expression relative to day 0 (D0). N = 3. *P < 0.01 relative to gels with 0.6 μ g/mL TGF- β 3. (b–d) GAG deposition by alcian blue staining also show comparable stain intensity for 0.6 and 0.4 μ g/mL TGF- β 3 doses (b, c), with lower intensity detected for 0.1 μ g/mL dose (d). (For interpretation of the references to colour in this figure legend, the reader is referred to the web version of this article.)

The higher delivery efficacy sustained long term without the need for repeated TGF- β 3 supplementation offers opportunity to reduce GF dose without compromising on biological outcomes. As such this method provides an efficient growth factor delivery system particularly in a 3D cell-encapsulated scaffold, with the potential to simultaneously deliver multiple factors. Furthermore, the potential of GO to ensure local delivery of biological cues is an attractive strategy worth further exploration for tissue engineering, in particular for regionally-specific MSC differentiation.

Declaration of Competing Interest

None.

Acknowledgements

The authors thank Mr Gian Fulgoni, president of North American Foundation for the University of Manchester, for his generous financial support on this project and Dr Mi Zhou's fellowship. This work was also partially funded by the European Union's 7th RTD Framework Program: Graphene Flagship project (FP7-ICT-2013-FET-F-604391) and has received funding from the European Union's Horizon 2020 research and innovation programme under grant agreement No 696656 (Graphene Flagship Core1).

The authors also acknowledge the Engineering and Physical Sciences Research Council (EPSRC) for supporting the work of Dr Jacek Wychowaniec of the Northwest Nanoscience Doctoral Training Centre (NOWNANO DTC), with an EP/G03737X/1 grant, and an EPSRC doctoral training award (DTA) from the School of Materials, University of Manchester. This research was also supported by the NIHR Biomedical Research Centre. The authors also acknowledge funding to support Dr Tom Hodgkinson from the Biotechnology and Biological Sciences Research Council (BBSRC); EPSRC; and Medical Research Council (MRC) (grant number MR/K026682/1) via the UK Regenerative Medicine Platform Hubs "Acellular Approaches for Therapeutic Delivery", as well as the MRC via a Confidence-in-Concept 2014 award to The University of

Manchester (MC_PC_14112 v.2) and the National Institute for Health Research Manchester Biomedical Research Centre.

The authors also thank Dr Aleksandr Mironov for his expert contribution on Bio-TEM, Mrs Sonal Patel for her expertise in histology staining, and Dr Zhengxin Cui for his contribution on rheology.

We thank the staff in the Faculty of Biology, Medicine and Health EM Facility, for their expertise and the Wellcome Trust for equipment grant support to the facility. The University of Manchester Bioimaging Facility microscopes used in this study were purchased with grants from the BBSRC, Wellcome Trust and the University of Manchester Strategic Fund. We also thank Dr Nigel Hodson for his expert advice and support concerning the use of the Multimode AFM and also the University of Manchester Bioimaging facility of which the AFM unit is part. Also, we are grateful to Mr Artur Filipe Rodrigues and Dr Leon Newman of the Nanomedicine Lab for their critical feedback and fruitful discussions concerning the contents of this manuscript.

Appendix A. Supplementary data

Supplementary data to this article can be found online at <https://doi.org/10.1016/j.actbio.2019.07.027>.

References

- [1] D.J. Hunter, D. Schofield, E. Callander, The individual and socioeconomic impact of osteoarthritis, *Nat. Rev. Rheumatol.* 10 (7) (2014) 437–441.
- [2] A. Chen, C. Gupte, K. Akhtar, P. Smith, J. Cobb, The Global Economic Cost of Osteoarthritis: How the UK Compares, *Arthritis* 2012 (2012).
- [3] C. Vinatier, C. Bouffi, C. Merceron, J. Gordanadze, J.M. Brondello, C. Jorgensen, P. Weiss, J. Guicheux, D. Noel, Cartilage Tissue Engineering: Towards a Biomaterial-Assisted Mesenchymal Stem Cell Therapy, *Curr. Stem Cell Res. Ther.* 4 (4) (2009) 318–329.
- [4] W. Zhang, H.W. Ouyang, C.R. Dass, J.K. Xu, Current research on pharmacologic and regenerative therapies for osteoarthritis, *Bone Res.* 4 (2016).
- [5] K.L. Spiller, S.A. Maher, A.M. Lowman, Hydrogels for the repair of articular cartilage defects, *Tissue Eng. Part B-Rev.* 17 (4) (2011) 281–299.
- [6] S. Sundelacruz, D.L. Kaplan, Stem cell- and scaffold-based tissue engineering approaches to osteochondral regenerative medicine, *Semin. Cell Dev. Biol.* 20 (6) (2009) 646–655.

- [7] P. M., M. J., B. B, Handbook of Medical and Healthcare Technologies, Springer, 2013.
- [8] F.J. O'Brien, Biomaterials & scaffolds for tissue engineering, *Mater. Today* 14 (3) (2011) 88–95.
- [9] K. Lee, E.A. Silva, D.J. Mooney, Growth factor delivery-based tissue engineering: general approaches and a review of recent developments, *J. R. Soc. Interface* 8 (55) (2011) 153–170.
- [10] Y. Ikada, Challenges in tissue engineering, *J. R. Soc. Interface* 3 (10) (2006) 589–601.
- [11] R. Krishnamurthy, M.C. Manning, The stability factor: importance in formulation development, (1389-2010 (Print)).
- [12] A.K.A. Silva, C. Richard, M. Bessodes, D. Scherman, O.W. Merten, Growth Factor Delivery Approaches in Hydrogels, *Biomacromolecules* 10 (1) (2009) 9–18.
- [13] A. Kumari, S.K. Yadav, S.C. Yadav, Biodegradable polymeric nanoparticles based drug delivery systems, *Colloids Surf. B-Biointerfaces* 75 (1) (2010) 1–18.
- [14] M.H. Sheridan, L.D. Shea, M.C. Peters, D.J. Mooney, Bioadsorbable polymer scaffolds for tissue engineering capable of sustained growth factor delivery, *J. Control. Release* 64 (1–3) (2000) 91–102.
- [15] J.I. Dawson, J.M. Kanczler, X.B.B. Yang, G.S. Attard, R.O.C. Oreffo, Clay Gels For the Delivery of Regenerative Microenvironments, *Advanced Materials* 23(29) (2011) 3304–+.
- [16] D.M.R. Gibbs, C.R.M. Black, G. Hulsart-Billstrom, P. Shi, E. Scarpa, R.O.C. Oreffo, J.I. Dawson, Bone induction at physiological doses of BMP through localization by clay nanoparticle gels, *Biomaterials* 99 (2016) 16–23.
- [17] I. Freeman, A. Kedem, S. Cohen, The effect of sulfation of alginate hydrogels on the specific binding and controlled release of heparin-binding proteins, *Biomaterials* 29 (22) (2008) 3260–3268.
- [18] M.E. Davis, P.C.H. Hsieh, T. Takahashi, Q. Song, S.G. Zhang, R.D. Kamm, A.J. Grodzinsky, P. Anversa, R.T. Lee, Local myocardial insulin-like growth factor 1 (IGF-1) delivery with biotinylated peptide nanofibers improves cell therapy for myocardial infarction, *PNAS* 103 (21) (2006) 8155–8160.
- [19] K.S. Novoselov, A.K. Geim, S.V. Morozov, D. Jiang, Y. Zhang, S.V. Dubonos, I.V. Grigorieva, A.A. Firsov, Electric field effect in atomically thin carbon films, *Science* 306 (5696) (2004) 666–669.
- [20] K. Tadyszak, J.K. Wychowaniec, J. Litowczenko, Biomedical applications of graphene-based structures, *Nanomaterials* 8 (11) (2018).
- [21] D. Chimene, D.L. Alge, A.K. Gaharwar, Two-Dimensional nanomaterials for biomedical applications: emerging trends and future prospects, *Adv. Mater.* 27 (45) (2015) 7261–7284.
- [22] M. Kalbacova, A. Broz, J. Kong, M. Kalbac, Graphene substrates promote adherence of human osteoblasts and mesenchymal stromal cells, *Carbon* 48 (15) (2010) 4323–4329.
- [23] T.R. Nayak, H. Andersen, V.S. Makam, C. Khaw, S. Bae, X.F. Xu, P.L.R. Ee, J.H. Ahn, B.H. Hong, G. Pastorin, B. Ozyilmaz, Graphene for controlled and accelerated osteogenic differentiation of human mesenchymal stem cells, *ACS Nano* 5 (6) (2011) 4670–4678.
- [24] J.F. Wang, J. Guo, J.S. Liu, L.M. Wei, G. Wu, BMP-functionalised coatings to promote osteogenesis for orthopaedic implants, *Int. J. Mol. Sci.* 15 (6) (2014) 10150–10168.
- [25] S.W. Crowder, D. Prasai, R. Rath, D.A. Balikov, H. Bae, K.I. Bolotin, H.J. Sung, Three-dimensional graphene foams promote osteogenic differentiation of human mesenchymal stem cells, *Nanoscale* 5 (10) (2013) 4171–4176.
- [26] N. Li, Q. Zhang, S. Gao, Q. Song, R. Huang, L. Wang, L. Liu, J. Dai, M. Tang, G. Cheng, Three-dimensional graphene foam as a biocompatible and conductive scaffold for neural stem cells, *Sci. Rep.* 3 (2013).
- [27] J. Kim, K.S. Choi, Y. Kim, K.T. Lim, H. Seonwoo, Y. Park, D.H. Kim, P.H. Chung, C. S. Cho, S.Y. Kim, Y.H. Chung, J.H. Chung, Bioactive effects of graphene oxide cell culture substratum on structure and function of human adipose-derived stem cells, *J. Biomed. Mater. Res. Part A* 101 (12) (2013) 3520–3530.
- [28] S.H. Li, J.J. Mulloor, L.Y. Wang, Y.W. Ji, C.J. Mulloor, M. Micic, J. Orbulescu, R.M. Leblanc, Strong and Selective Adsorption of Lysozyme on Graphene Oxide, *ACS Appl. Mater. Interfaces* 6 (8) (2014) 5704–5712.
- [29] X. Zou, S. Wei, J. Jasensky, M. Xiao, Q. Wang, C.L. Brooks Iii, Z. Chen, Molecular interactions between graphene and biological molecules, *J. Am. Chem. Soc.* (2017).
- [30] W.C. Lee, C.H.Y.X. Lim, H. Shi, L.A.L. Tang, Y. Wang, C.T. Lim, K.P. Loh, Origin of enhanced stem cell growth and differentiation on graphene and graphene oxide, *ACS Nano* 5 (9) (2011) 7334–7341.
- [31] H.H. Yoon, S.H. Bhang, T. Kim, T. Yu, T. Hyeon, B.S. Kim, Dual roles of graphene oxide in chondrogenic differentiation of adult stem cells: cell-adhesion substrate and growth factor-delivery carrier, *Adv. Funct. Mater.* 24 (41) (2014) 6455–6464.
- [32] A. Paul, A. Hasan, H. Al Kindi, A.K. Gaharwar, V.T.S. Rao, M. Nikkhah, S.R. Shin, D. Krafft, M.R. Dokmeci, D. Shum-Tim, A. Khademhosseini, Injectable Graphene Oxide/Hydrogel-Based Angiogenic Gene Delivery System for Vasculogenesis and Cardiac Repair, *ACS Nano* 8 (8) (2014) 8050–8062.
- [33] J. Wang, C.H. Liu, Y. Shuai, X.Y. Cui, L. Nie, Controlled release of anticancer drug using graphene oxide as a drug-binding effector in konjac glucomannan/sodium alginate hydrogels, *Colloids Surf. B-Biointerfaces* 113 (2014) 223–229.
- [34] R. Rauti, N. Lozano, V. Leon, D. Scaini, M. Musto, I. Rago, F.P.U. Severino, A. Fabbro, L. Casalis, E. Vazquez, K. Kostarelos, M. Prato, L. Ballerini, Graphene oxide nanosheets reshape synaptic function in cultured brain networks, *ACS Nano* 10 (4) (2016) 4459–4471.
- [35] S.P. Mukherjee, N. Lozano, M. Kucki, A.E. Del Rio-Castillo, L. Newman, E. Vazquez, K. Kostarelos, P. Wick, B. Fadeel, Detection of endotoxin contamination of graphene based materials using the TNF-alpha expression test and guidelines for endotoxin-free graphene oxide production, *PLoS One* 11 (11) (2016).
- [36] Y. Nagai, L.D. Unsworth, S. Koutsopoulos, S. Zhang, Slow release of molecules in self-assembling peptide nanofiber scaffold, *J. Control. Release* 115 (1) (2006) 18–25.
- [37] J. Siepmann, N.A. Peppas, Modeling of drug release from delivery systems based on hydroxypropyl methylcellulose (HPMC), *Adv. Drug Deliv. Rev.* 64 (2012) 163–174.
- [38] J. Pellaud, U. Schote, T. Arvinte, J. Seelig, Conformation and self-association of human recombinant transforming growth factor-beta 3 in aqueous solutions, *J. Biol. Chem.* 274 (12) (1999) 7699–7704.
- [39] K.L. Burrow, J.A. Hoyland, S.M. Richardson, Human adipose-derived stem cells exhibit enhanced proliferative capacity and retain multipotency longer than donor-matched bone marrow mesenchymal stem cells during expansion *In Vitro*, *Stem Cells Int.* 2017 (2017).
- [40] K.J. Livak, T.D. Schmittgen, Analysis of relative gene expression data using real-time quantitative PCR and the 2^(-Delta Delta C) method, *Methods* 25 (4) (2001) 402–408.
- [41] W.C. Johnson, Protein secondary structure and circular-dichroism – a practical guide, *Proteins-Struct. Funct. Genet.* 7 (3) (1990) 205–214.
- [42] J.K. Wychowaniec, M. Iliut, M. Zhou, J. Moffat, M.A. Elsayy, W.A. Pinheiro, J.A. Hoyland, A.F. Miller, A. Vijayaraghavan, A. Saiani, Designing peptide/graphene hybrid hydrogels through fine-tuning of molecular interactions, *Biomacromolecules* 19 (7) (2018) 2731.
- [43] H. Shen, M. Liu, H.X. He, L.M. Zhang, J. Huang, Y. Chong, J.W. Dai, Z.J. Zhang, PEGylated graphene oxide-mediated protein delivery for cell function regulation, *ACS Appl. Mater. Interfaces* 4 (11) (2012) 6317–6323.